AD-A098 111 CALIFORNIA INST OF TECH PASADENA GRADUATE AERONAUTIC--ETC F/G 20/4
DYNAMICS OF TURBULENT VORTEX RINGS.(U)
JAN 81 B STURTEVANT
F49620-77-C-0107
UNCLASSIFIED GALCIT-134-(B) AFOSR-TR-81-0400 NL

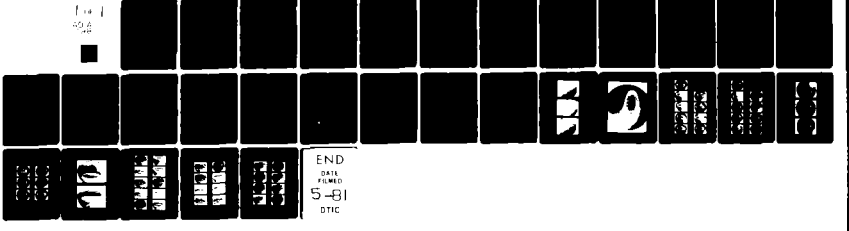

END
DATE FILMED
5-81
DTIC

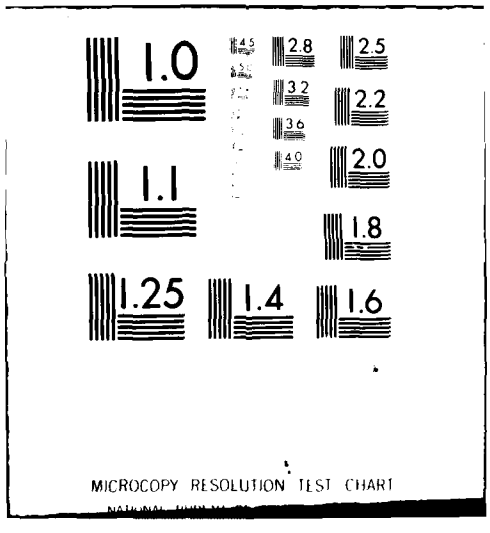
1.0
1.1
1.25
1.4
1.6
1.8
2.0
2.2
2.5
2.8
3.2
3.6
4.0
MICROCOPY RESOLUTION TEST CHART

FINAL SCIENTIFIC REPORT

Contract Number F49620-77-C-0107

DYNAMICS OF TURBULENT VORTEX RINGS

1 May 1978 - 30 April 1980

Submitted by:

B. Sturtevant

B. Sturtevant
Principal Investigator
Professor of Aeronautics

Graduate Aeronautics Laboratories
California Institute of Technology
Pasadena, California 91125

31 January 1981

"Qualified requestors may obtain additional copies from the Defense Technical Information Service."

UNCLASS D

SECURITY CLASSIFICATION OF THIS PAGE (When Data Entered)

REPORT DOCUMENTATION PAGE

READ INSTRUCTIONS BEFORE COMPLETING FORM

1. REPORT NUMBER: AFOSR-TR-81-0400	2. GOVT ACCESSION NO.: AD-A098111
3. RECIPIENT'S CATALOG NUMBER	
4. TITLE (and Subtitle): DYNAMICS OF TURBULENT VORTEX RINGS	5. TYPE OF REPORT & PERIOD COVERED: FINAL, 1 May 78 — 30 Apr 80
6. PERFORMING ORG. REPORT NUMBER: GALCIT-134-(B)	
7. AUTHOR(s): BRADFORD STURTEVANT	8. CONTRACT OR GRANT NUMBER(s): F49620-77-C-0107
9. PERFORMING ORGANIZATION NAME AND ADDRESS: CALIFORNIA INSTITUTE OF TECHNOLOGY, GRADUATE AERONAUTICAL LABORATORIES, PASADENA, CA 91125	10. PROGRAM ELEMENT, PROJECT, TASK AREA & WORK UNIT NUMBERS: 61102F, 2307/A4
11. CONTROLLING OFFICE NAME AND ADDRESS: AIR FORCE OFFICE OF SCIENTIFIC RESEARCH/NA, BLDG. 410, BOLLING AIR FORCE BASE, WASHINGTON D.C. 20332	12. REPORT DATE: 31 JAN [redacted]81
	13. NUMBER OF PAGES: 22
14. MONITORING AGENCY NAME & ADDRESS (if different from Controlling Office): 31	15. SECURITY CLASS. (of this report): UNCLASSIFIED
	15a. DECLASSIFICATION DOWNGRADING SCHEDULE

16. DISTRIBUTION STATEMENT (of this Report)

APPROVED FOR PUBLIC RELEASE; DISTRIBUTION UNLIMITED

17. DISTRIBUTION STATEMENT (of the abstract entered in Block 20, if different from Report)

18. SUPPLEMENTARY NOTES

19. KEY WORDS (Continue on reverse side if necessary and identify by block number)

VORTEX RINGS
TURBULENT SHEAR FLOWS

20. ABSTRACT (Continue on reverse side if necessary and identify by block number)

One of the major challenges facing engineers who deal with complicated flow systems is the question of how to analyze flow fields containing complex distributions of vorticity. Such flow fields occur in boundary layers and other shear flows and also in applications where mixing is a prime consideration, such as in combustors, chemical lasers, etc. It is often necessary to know something about the scale and geometry of the flow field, in addition to the mixing and transport. Unfortunately, vortex interactions are inherently long range and no local theory can yield the geometry of the flow or the distributio

DD FORM 1 JAN 73 1473 EDITION OF 1 NOV 65 IS OBSOLETE

UNCLASSIFIED 157700

SECURITY CLASSIFICATION OF THIS PAGE (When Data Entered)

of the vorticity at any given location. Consequently, there is presently no approximate theory for treating vortex flows of complicated geometry. In order to provide information about the processes that are important in vortex flows, and to provide guidance for the development of theoretical models of these flows, it is important that experiments exploring the fundamental behavior of simple vortex flows be carried out.

Turbulent vortex rings in air at Reynolds numbers up to 600,000 have been studied by schlieren flow visualization. Both the bulk fluid in the vortex rings and small tracer volumes in the rings have been tagged thermally for visualizing the flow processes within and on the boundaries of the vortex. The fundamental wave-like instability on the cores of vortex rings has been observed to grow to maximum amplitude and then decay, instead of breaking and developing into turbulence, as had previously been observed in dye-visualization experiments in water. This observational difference may be due to the fact that schlieren visualization exhibits the correct instantaneous state of the flow, while dye visualization is subject to the influence of the entire history of the flow between the time of dye injection and the instant of observation. In particular, transport of dye into the outer turbulent regions of a vortex ring may be mistaken for the breaking of instability waves. The development of rather large structures on the boundary between the vortex ring and the outer fluid is seen to be the cause of the ejection of vortex fluid into the wake and entrainment of external fluid into the vortex. These structures develop from smooth disturbances on the boundaries of young rings. Apparently, during formation a vortex ring progresses through several developmental stages, including roll up, generation of chaotic fluctuations, core instability and subsequent restabilization, all of which are transient and presumably depend on the initial conditions and method of generation of the vortex.

The fact that in the present experiments substantially different behavior has been observed in vortex rings of high Reynolds number and with thin cores than had previously been observed in water with rings of lower Re and with thick cores emphasizes that the extrapolation of results from small-scale laboratory experiments to full scale should be approached with caution. It is important that the implications of the preliminary observations made in the present work be explored in more detail and that the study of thin-cored vortices be continued.

FINAL SCIENTIFIC REPORT
Office of Scientific Research, The United States Air Force
Contract Number F49620-77-C-0107

DYNAMICS OF TURBULENT VORTEX RINGS

1. INTRODUCTION

One of the major challenges facing engineers who deal with complicated flow systems is the question of how to analyze flow fields containing complex distributions of vorticity. Such flow fields occur in boundary layers and other shear flows and also in applications where mixing is a prime consideration, such as in combustors, chemical lasers, etc. It is often necessary to know something about the scale and geometry of the flow field, in addition to the mixing and transport. In this connection it is interesting to compare the methods available for analyzing vortex flows with those used to treat another flow of fundamental importance in fluid mechanics, namely wave propagation. In the latter case it is true that, at least insofar as the geometry and amplitude of wave fronts is concerned, it is possible to find approximate solutions by only local, geometrical reasoning, using the so-called theory of geometrical optics or its non-linear equivalent, shock dynamics. On the other hand, there is no local approximation available for vortex flows. Due to the fundamental property expressed by the Biot-Savart law, vortex interactions are inherently long range and no local theory can yield the geometry of the flow or the distribution of the vorticity at any given location. Consequently, there is presently no approximate theory for treating vortex flows of complicated geometry.

In order to provide information about the processes that are important in vortex flows, and to provide guidance for the development of theoretical models of these flows, it is important that experiments exploring the fundamental behavior of simple vortex flows be carried out. Relatively simple flows should be examined, so that there will be some hope that the important processes that must be retained in any theoretical model of vortex flows, and the unimportant ones which can be neglected, will be apparent. On the other hand, in order to insure that experiments contain all the processes which occur in large-scale vortex flows in applications, it is important that a significant range of physical scales occurs in the flow; that is, that the flow be at high Reynolds number, and that only the smallest scales be affected by viscosity. The processes which should be examined and characterized by the experiments include the stability of vortex flows, turbulence production and dissipation, development and/or decay of geometrical structures in the flows, and entrainment and mixing.

One vortex flow which occurs in many flow problems and has

been studied rather extensively is the turbulent vortex ring. Vortical structures that can be catagorized as vortex rings occur in smoke rings, as the starting vortices behind impulsively accelerated bluff bodies and in gun muzzle blasts. Vortex rings are the axially-symmetric analog of wingtip trailing vortices and, because the vortex lines are closed, are much easier to produce in the laboratory (Barker & Crow 1977). The vortex ring is also known to exhibit many of the features of more complicated flows, including long-range interactions between vortex elements, yet it is a relatively well-defined entity, being confined to a finite region of space, and is therefore convenient to study. The study of interactions between vortex rings also promises to yield important information in this connection.

Two parameters that are important in scaling laboratory-generated vortex rings to large scale are the Reynolds number, $Re = \Gamma/\nu$ (where Γ is the circulation about the core of the ring, and ν is the kinematic viscosity) and the ratio R/a of the ring diameter, $2R$, to the diameter, $2a$, of the rotational core of the vortex ring. For young rings a depends on the method by which the vortex was generated, and for flows of interest is larger than the viscous core radius $\delta \sim \nu t$, where t is the age of the vortex. The Reynolds number, as defined above, is not an especially useful measure of the effects of viscosity because it can only be expressed as the square of the ratio of the ring diameter to the viscous core diameter times the number of ring diameters the ring has travelled in its lifetime, $(R/\delta)^2 (Ut/R)$. Nevertheless, it should be emphasized that, in order to be useful for understanding large-scale vortex flows in applications, laboratory-generated vortex rings should have both high Reynolds number and $R/a >> 1$.

A model for the velocity profile and vorticity distribution in two-dimensional laminar vortices which includes the effects of viscosity near the center has been described by Saffman (1978). A qualitative picture of the streamlines in the corresponding axially-symmetric case (vortex ring) is sketched in the vortex-fixed frame of reference in figure 1. Note that the vortex structure is closed by a dividing streamline which begins at the front stagnation point and ends at the rear stagnation point. It will become apparent later in this report that the processes which occur in laboratory-generated vortex rings near this boundary between the outer flow and the vortex appear to be very important in determining the behavior of the vortex.

Vortex rings with Reynolds numbers of order 60,000 have been studied rather extensively in water using dye visualization. Information has been obtained about methods for production of vortex rings using impulsive jets and the effect on the structure of the

vortex of nozzle geometry and the fluid velocity history in the ring generator (Maxworthy 1977, Didden 1979). It has been demonstrated that vortex rings are amazingly persistent structures and decay only very slowly. The decay is by the action of viscosity near the core of the ring, where the gradients are largest, and by loss of fluid to a "wake" by "de-entrainment", a process that is not at all understood. Indeed, little is known about turbulence production and dissipation, and entrainment and mixing in vortex rings. Unfortunately, the experiments in water have all been at relatively low Reynolds number and the rotational core diameter has been rather large, $a \sim R$.

A good deal has been learned about the stability of laminar vortex rings, although all of the possible mechanisms for generation of turbulence in vortex rings have not been delineated. The theory by Widnall, Bliss and Tsai (1974) of a fundamental wavelike instability on the core of vortex rings, which is caused by the response of a vortex element to straining by the velocity field of vortex elements opposite in the ring, has been effectively substantiated by experiment. It is interesting that in all of the experiments to date the fundamental core instability seems to first appear at a distance of order 5 diameters from the mouth of the vortex generator. One important question that has not yet been satisfactorily resolved is that of transition to turbulence in vortex rings. One school of thought (e.g., Maxworthy 1977) holds that the mechanism for transition starts first with the appearance of the core instability and then progresses through a stage of non-linear growth of disturbances on the core of the ring, including "breaking" of the instability waves as in vortex breakdown, to a chaotic velocity field distributed through-out the entire vortex ring. However, in the present experiments turbulent vortex rings have been observed in all cases, even before the appearance of instability waves on the core.

It may be apparent from the above discussion that understanding of the nature of turbulent vortex rings is still very incomplete. Indeed, the meaning of the term "turbulent vortex ring" has not been defined in detail and, at best, it can only be regarded as a label for a chaotic flow field observed in flow-visualizations experiments. The difficulty, of course, stems mainly from the fact that a ring vortex is a three-dimensional rotational flow, so the processes of turbulence production and transport can be very complicated. It is extremely important that experiments be directed at finding ways to simplify this picture. It is necessary to have better information about the distribution of turbulence in vortex rings, about the degree of entrainment into and loss of mass from the rings, and about momentum transport.

Because of the difficulty of experiments, it will no doubt be some time before any complete understanding of even this apparently simple example of vortex flow is obtained. In a laboratory-fixed frame of reference the flows are transient, and, as with all vortex flows, insertion of probes into the flow can cause severe perturbation of the flow field. Thus, it is essential that non-intrusive (optical) techniques be used, even though many optical methods suffer from pathlength averaging. Furthermore, in air, where the highest Reynolds numbers can be achieved, it is impossible to use laser Doppler velocimetry because dust particles are spun out of the flow by centrifugal acceleration. Therefore, new techniques must be developed in order to answer the questions posed above.

2. EXPERIMENTS

An experimental program to study the behavior of very-high-Reynolds-number thin-cored vortex rings in air has been initiated at GALCIT and preliminary results have been obtained. The Reynolds numbers of the rings studied in these experiments range from 120,000 to 600,000. New methods utilizing shock-tube techniques have been used to generate thin-cored vorticies, and unique methods of flow visualization have been used to obtain high-speed photcgraphs of the instantaneous flow field. A new method has been developed for tagging volumes of fluid within the vortex ring in order to study their deformation and dispersion. These new methods have led to a somewhat different picture of the behavior of turbulent vortex rings than had previously been the case.

2.1 Vortex Ring Generator

Most methods for producing vortex rings involve the generation of a short pulse of fluid at the mouth of a tube or orifice. The diameter of the orifice determines the diameter of the vortex ring. The length of the slug of gas ejected from the mouth of the vortex generator determines the diameter of the rotational core of the vortex ring, because it is the cylindrical shear layer on the perimeter of the slug that rolls up to produce the core of the ring. Thus, in order to generate thin-cored vortex rings of high Reynolds number, it is important that a relatively short slug of fluid be ejected at high velocity. From this point of view, the optimal vortex ring generator is an open-mouthed shock tube (Elder & deHass 1952) and such a device is used in the present experiments. The operation of the generator is indicated schematically in figure 2. The shock tube is 7.2 cm in diameter and 1.4 m long. The initial shock wave S generated by the rupture of the diaphragm accelerates the fluid in the tube to the right of the diaphragm. The leading edge of the slug of fluid which emerges from the open mouth of the tube immediately after passage of the shock wave is indicated by the

right-most dashed line in figure 2. The expansion wave E which propagates into the high-pressure gas (usually helium at 20 psig in our experiments) in the driver section reflects from the end wall of the shock tube and decelerates the fluid in the tube to rest. Therefore, this wave limits the length of the ejected slug. While the fluid is issuing from the mouth of the tube the shear layer rolls up and forms the vortex ring. Subsequently, the ring moves away from the tube by its own induced drift velocity. Drift velocities observed in the present experiments range from 16 to 55 m/s. It is interesting that the vortex also sees its image in the generator tube and in some cases can be ingested back into the tube. Motivated by our work, Sheffield (1977) has analyzed this problem, and Didden (1979) has published measurements of the effect. Reflected waves from the mouth of the tube propagate back and forth inside the tube during and after the formation of the vortex, but in our experiments the vortex has traveled sufficiently far before the first reflected wave returns to the mouth of the tube that it is little perturbed.

If such a shock-tube vortex generator is used, the length of the ejected slug of fluid, and therefore the diameter of the rotational core of the ring, is determined by the length of the driver section of the shock tube. In the present experiments, vortex rings with the ratio of ring diameter to core diameter R/a of order 10 have been generated. In practice, as the length of the driver section is increased both the diameter of the rotational core and strength of the vortex increase.

The shock-tube method of generating vortex rings has the advantage that the flow field in the tube is well-defined and almost perfectly uniform. In effect, the shock tube uses the potential energy stored in pressurized gas to accelerate (and later decelerate) a fluid impulsively, rather than to use a force applied to a piston to do work on the fluid, as with more conventional vortex-ring generators. Consequently, much higher fluid velocities and accelerations can be achieved. The shape of the velocity history generated by the shock tube is ideally of top-hat profile.

2.2 Flow Visualization

In the present experiments the vortex rings are visualized by schlieren photography. The core of the vortex is clearly visualized by this method due to the density gradients caused by the very large rotational velocities near the center of the vortex. It is important that, with this method of visualization, a view of the flow at one instant is obtained, while with dye visualization the effects of transport and mixing which occur during the period after the dye is injected alter the visualization. In the present experiments additional visualization of the flow field is provided by slightly pre-cooling the air which is ejected from the shock tube and is subsequently ingested into the vortex ring, thus distinguishing it from the surrounding ambient fluid. This method is analogous to dye injection, and the cool fluid inside the ring eventually mixes with the warmer surrounding fluid. Figure 3 shows a schematic plan view of the schlieren apparatus and vortex ring generator. The vorticies are viewed both from the side ($\theta = 0$) and obliquely ($15 < \theta < 30$).

2.3 Laser Spark Passive Tracer Technique

It has proven desirable to extend the methods of flow visualization described above so that motion within the vortex ring during any given stage in its development may be studied. For this purpose, a new technique has been developed for thermally tagging small volumes of fluid within a flow field for observation by the schlieren apparatus. In this case a volume of approximately 1 cm diameter, is heated by focusing a pulsed CO_2 laser on a point located within the vortex ring. The hot, rarefied tracer fluid is visible by the schlieren apparatus. The layout of the apparatus is indicated in Figure 4. This approach is analogous to injecting dye into the vortex at one location and at one instant, but has the advantage that it is non-intrusive.* Note that with this method the tagged fluid is slightly <u>lighter</u> than the surrounding fluid so that in a rotational flow it spins <u>inward</u> toward the center! Of course the effect of this motion must in any quantitative measurements be estimated and accounted for, but at least the tagged fluid moves <u>toward</u> the region of most interest rather than away from it, as is the case with dust particles that might be used for laser Doppler measurements.

---

* Actually, because the power of the CO_2 laser is marginal, it has been found necessary, in order to insure repeatable initiation of the spark, to stretch a long, very thin (0.005 in. dia.) wire so that it passes through the focal point.

Unfortunately, the laser-spark-tracer technique has proven not to be as useful for quanitative measurements as had been anticipated. Apparently, during the initiation of the spark and the heating of the fluid, outward acceleration of the gases is sufficient to cause Rayleigh-Taylor instability. Schlieren photographs of the hot fluid microseconds after the spark show a pronounced fingered structure. The heated gas rapidly becomes turbulent and mixes with its surroundings within 20 ms! This behavior was completely unexpected. Figure 5 is a schlieren photograph of the tracer fluid in still air at about the time after spark initiation at which we would wish to use it for flow measurements. (Δt is the time between the spark and the schlieren photograph.) The white spot at the center is caused by stray radiation from the spark. The mean diameter of the tracer fluid grows at a speed of approximately 9 m/s and the fluid is clearly turbulent. However, despite the unpleasant departure from ideal behavior, it is possible to use the spark-generated tracer fluid to study portions of the flow field in which mixing and dispersion is much more rapid than that which occurs naturally in the tracer.

3. RESULTS

3.1 Schlieren Visualization.

Figure 6 is a schlieren photograph of a vortex ring that has propagated 6.6 diameters from the vortex generator, showing the fundamental wave-like instability on the core of the ring. This ring was produced in the shock tube with a driver of length 15 cm. The schlieren method of visualization is clearly advantageous for photographing the core instability, because it is sensitive to the large density gradients that occur at the core. It is well known (Saffman 1978) that the number of instability waves which form on the core of a vortex scales with the inverse of the core diameter, 1/a. A large number of waves therefore signifies a very thin core; in figure 5 there are 22 waves. Figure 7 shows a complete sequence of photographs of vortex rings as they appear at different distances from a vortex generator. The behavior of the core instability in this sequence is quite different than what would be expected from the results of previous experiments with dye visualization in water. In particular, it can be seen that the amplitude of the instability waves does get rather large at about $x/D = 6$ (x is the axial distance from the vortex generator and D is the diameter of the shock tube), but then it does not continue to grow unboundedly, break and eventually degenerate into chaotic behavior, but, instead, simply decays in magnitude, disappearing altogether by $x/D = 40$. Evidently, the vorticity distribution in all laboratory-generated vortex rings reported so far is such that the rings are unstable to perturbations of the core, but apparently in the present experiments

the vorticity becomes sufficiently redistributed at later times that the rings subsequently become stable. In this connection it is very important that, for the shortest driver length (2.5 cm) studied in these experiments, no core instability is observed; this is the first time such behavior has been reported.

Figure 8 shows the behavior of a vortex generated by a 10 cm long driver. That the core is substantially thinner than for the 15 cm driver is seen by the fact that in this case there are approximately 28 waves on the core. Once again, the core instability reaches maximum amplitude at x/D = 6 and subsequently decays. Finally, figure 9 shows a vortex ring generated using a 5 cm long driver. This ring exhibits similar behavior, with the maximum amplitude of instability occurring at x/D = 6, but the subsequent decay proceeds much more rapidly. There are approximately 42 waves on the core of this ring!

3.2 Cooled-Gas Visualization

In order to better visualize the flow in the outer portions of the vortex ring near the dividing streamline, the fluid which is ingested into the vortex ring during formation of the vortex has been cooled by pre-chilling the walls of the shock tube. In this section we discuss flow-visualization schlieren photographs obtained by this technique.

Figure 10 shows, in oblique view, the behavior of a vortex ring generated with the 15 cm long driver. By the time the vortex has propagated 40 diameters from the vortex generator the cooled fluid ingested into the ring has mixed completely with warmer fluid entrained from the outside, but, before this time, a great deal of information about the flow field can be obtained from this method of flow visualization. In the first photograph of figure 10 (x/D = 1.7) the boundary between the vortex ring and the outer fluid is sharply defined. Dark circumferential rings extend around the interface dividing the vortex from the external fluid. These lines are suggestive of a wavy, unstable shear layer at the interface. The column of fluid seen behind the vortex ring at this close-in station is not a wake but is fluid ejected from the shock tube which has not been ingested into the vortex ring. In the second photograph (x/D = 3.1), the circumferential lines on the external interface have distorted and have developed a three-dimensional irregularity. The ring now trails a thin wake.

At x/D = 4.5 the flow inside the ring seems to be fully turbulent. Disturbances on the boundary of the ring protrude into the surrounding fluid and, after being convected along the boundary to the rear of the ring, seem to grow almost explosively outward

from the rearward surface of the ring. Apparently, this is a mechanism for ejection of fluid into the wake of the vortex ring, because in this photograph, and in subsequent ones, the wake thickens very rapidly. The rapid growth of disturbances on the interface at the rear of the vortex ring appears to be the mechanism not only for ejecting ring fluid into the wake but also for entraining external fluid into the ring, because, after $x/D = 6.0$, mixing within the ring becomes so strong that the photographs rapidly loose their contrast. By $x/D = 6.0$ the spatial distribution of the inhomogeneities within the ring seems to have become relatively homogeneous and isotropic. It is noteworthy that this state of fully-developed turbulence is reached just before the instability waves on the core of the ring reach substantial amplitude. Though the relationship between the core instability and the turbulence in the ring is not at all clear, it is certainly apparent from these photographs that substantial three-dimensional random, unsteady motion (turbulence) occurs within the ring before there are any signs of the fundamental core instability.

3.3 Laser Spark Tracer

Figure 11 shows two different views of the distortion of a laser spark tracer by the flow field inside a vortex ring only 200 μs after spark initiation. In both cases (and in all subsequent photographs) the spark is positioned in a plane of symmetry at a location sightly inside and upstream of the vortex core. The white spot from the spark indicates the position on the wire, but not on the moving vortex ring, where the spark occurred. The wire extends far enough in both directions out of the plane of the photograph that the supports visible in the photograph are well away from the vortex ring. The rate of strain at the location in the ring occupied by the tracer in figure 11 is of order $10^4 sec^{-1}$.

Figure 12 shows the change of the appearance of the spark tracer with increasing time after spark initiation. It may be seen that at large times (last two photographs) some of the tracer fluid has even been ejected into the wake of the vortex ring near the original location at which the spark occurred.

Figure 13 shows that the behavior of the spark tracer in a vortex that has propagated further from the vortex generator is essentially the same as already seen in figure 12, despite the fact that in figure 13 the fundamental core instability is fully developed. Apparently the small scale turbulence in the ring is not greatly affected by the core instability, and vice versa.

The shortest driver that has been used in these experiments is 2.5 cm long. This particular driver performs anomalously in two

respects. First, as mentioned above, no wavelike instability develops on the cores of vortex rings generated by this driver. Second, as seen in figure 14, the (less dense) spark tracer fluid rapidly intrudes into the core of the vortex and races axially along the core in both directions at nearly acoustic velocity! The tracer fluid that has reached locations in the core remote from the point of the spark mixes rather rapidly, so that at late times only the tracer fluid near the point of origin is visible.

4. CONCLUSIONS

Turbulent vortex rings in air at Reynolds numbers up to 600,000 have been studied by schlieren flow visualization. Both the bulk fluid in the vortex rings and small tracer volumes in the rings have been tagged thermally for visualizing the flow processes within and on the boundaries of the vortex. The fundamental wave-like instability on the cores of vortex rings has been observed to grow to maximum amplitude and then decay, instead of breaking and developing into turbulence, as had previously been observed in dye-visualization experiments in water. This observational difference may be due to the fact that schlieren visualization exhibits the correct instantaneous state of the flow, while dye visualization is subject to the influence of the entire history of the flow between the time of dye injection and the instant of observation. In particular, transport of dye into the outer <u>turbulent</u> regions of a vortex ring may be mistaken for the breaking of instability waves. In this connection it is important to note that in the present experiments the flow in the vortex rings is observed to be turbulent <u>before</u> the development of the core instability.

The development of rather large structures on the boundary between the vortex ring and the outer fluid is seen to be the cause of the ejection of vortex fluid into the wake and entrainment of external fluid into the vortex. These structures develop from smooth disturbances on the boundaries of young rings, and this suggests that the flow on the boundary is a shear flow, with (in the vortex-fixed frame) relatively low-velocity fluid inside the ring and high velocity fluid outside. This is in contrast to the conventional model of a non-decaying vortex ring, (figure 1) in which there is simply a dividing streamline at the boundary and in which the circumferential velocity increases monatonically toward the core of the vortex. Apparently, during formation a vortex ring progresses through several developmental stages, including roll up, generation of chaotic fluctuations, core instability and subsequent restabilization, all of which are transient and presumably depend on the initial conditions and method of generation of the vortex. On the other hand, a mature vortex ($x/D \gtrsim 10$) seems to change relatively slowly.

The fact that in the present experiments substantially different behavior has been observed in vortex rings of high Reynolds number and with thin cores than had previously been observed in water with rings of lower Re and with thick cores emphasizes that the extrapolation of results from small-scale laboratory experiments to full scale should be approached with caution. It is important that the implications of the preliminary observations made in the present work be explored in more detail and that the study of thin-cored vortices be continued.

5. REFERENCES

Barker, S.J. & Crow, S.C. 1977 J. Fluid Mech. 62, 659.

Elder, F.K., Jr. & deHaas, N. 1952 J. App. Phys. 23, 1065.

Didden, N. 1979 ZAMP 30, 101.

Maxworthy, T. 1977 J. Fluid Mech. 81, 465.

Saffman, P.G. 1978 J. Fluid Mech. 84, 625.

Sheffield, J.S. 1977 Phys. Fluids 20, 543.

Widnall, S.E., Bliss, D.B. & Tsai, C-Y. 1974 J. Fluid Mech. 66, 35.

6. LIST OF PUBLICATIONS

"On Generation of Slender-Core Vortex Rings." by V.A. Kulkarny. Bull. Am. Phys. Soc. 21, 1223 (1976).

"Experimental Observations of Slender-Core Vortex Rings." by V.A. Kulkarny. Bull. Am. Phys. Soc. 23, 988 (1978).

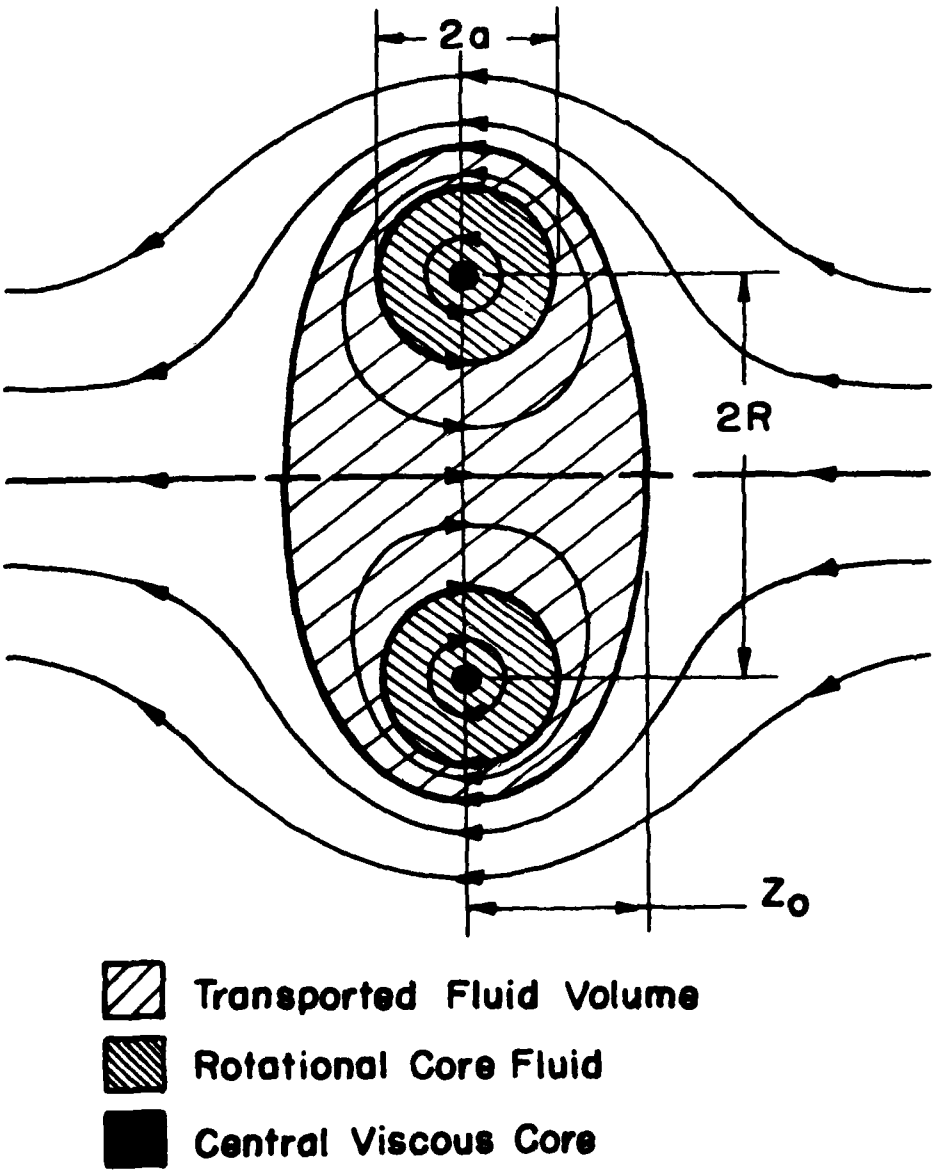

Figure 1. Schematic Diagram of a Vortex Ring

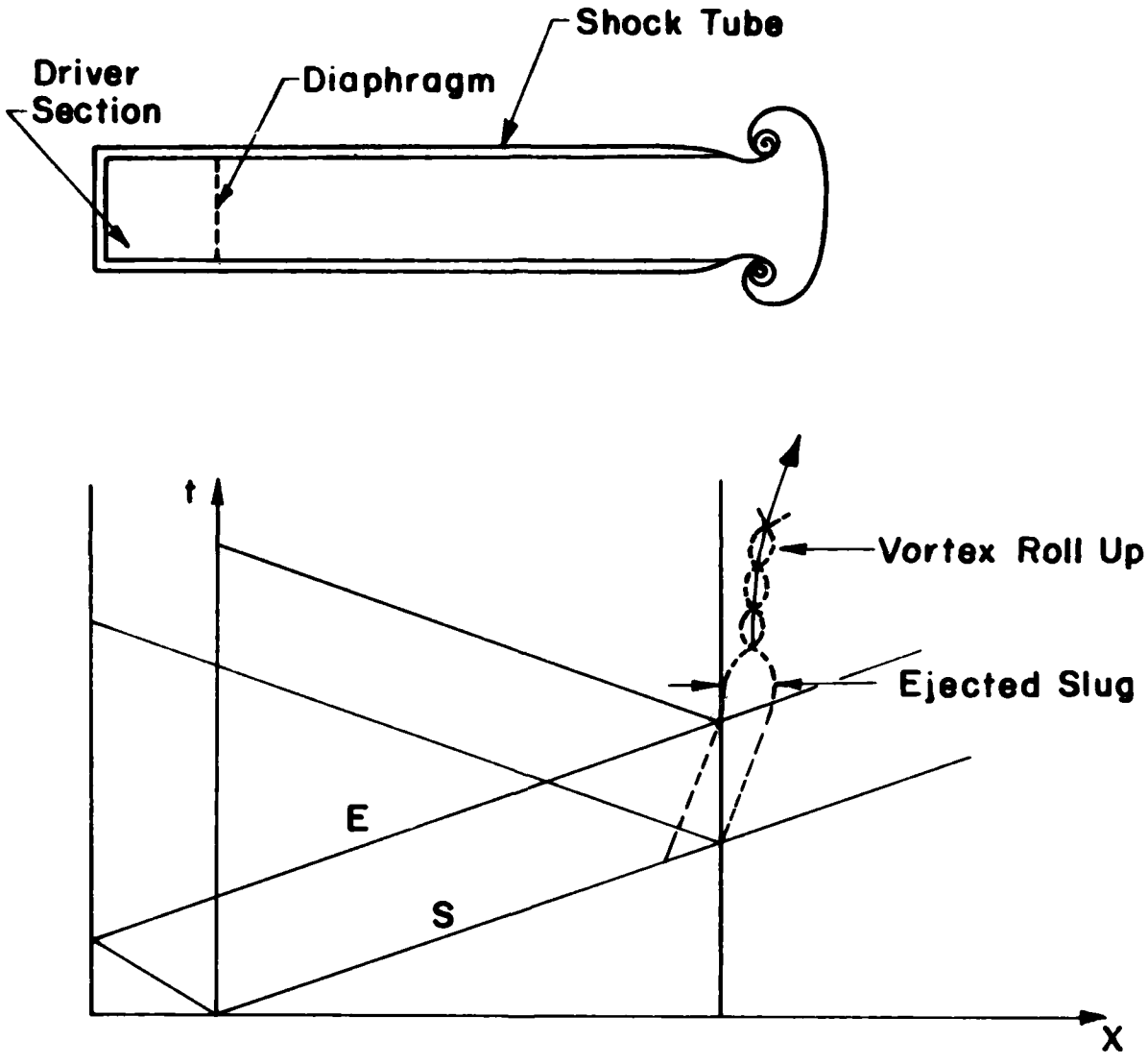

Figure 2. Schematic and Wave Diagram of the Operation of a Shock-Tube Vortex Generator

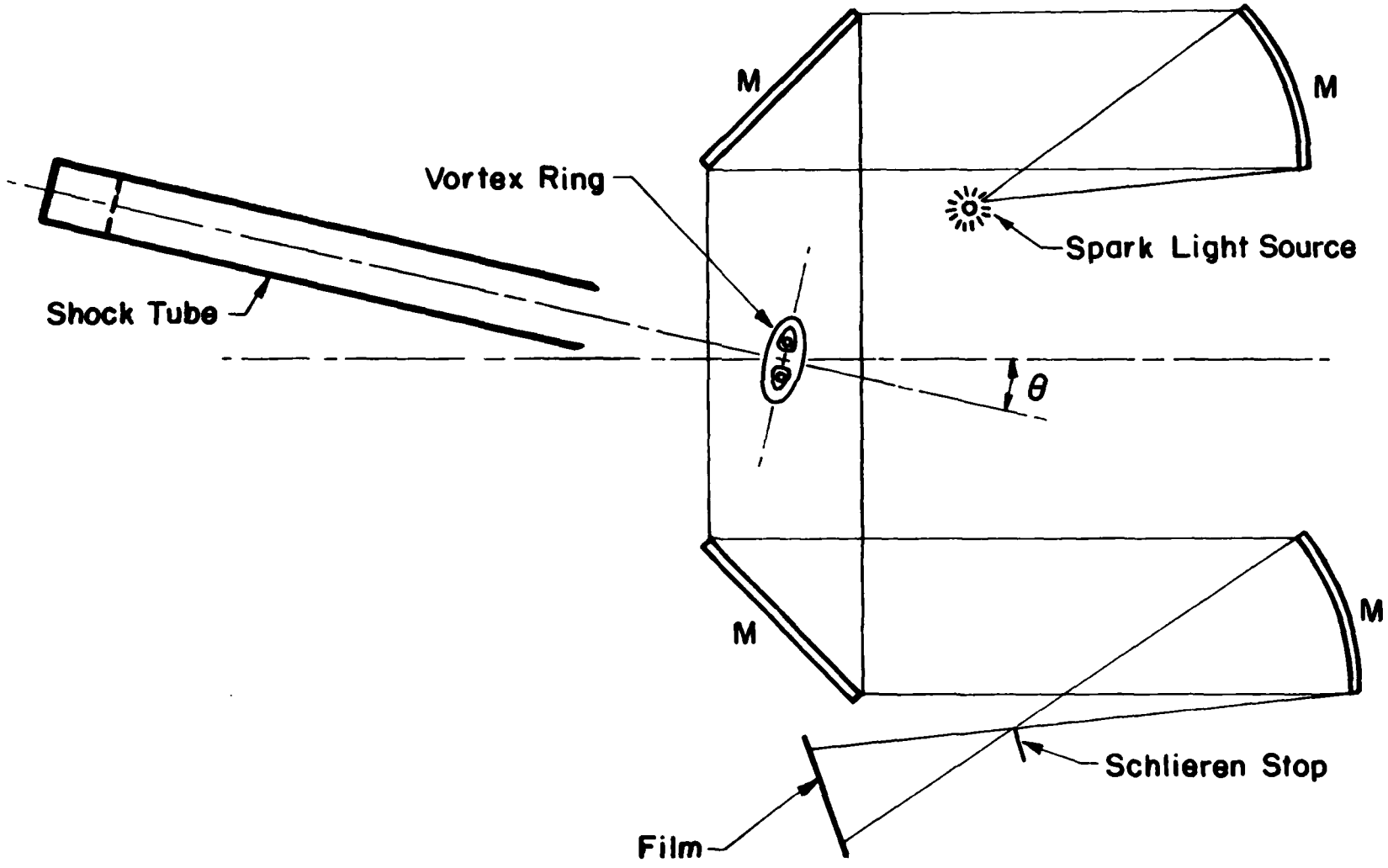

FIGURE 3 SCHEMATIC PLAN VIEW OF SHOCK TUBE AND SCHLIEREN SYSTEM

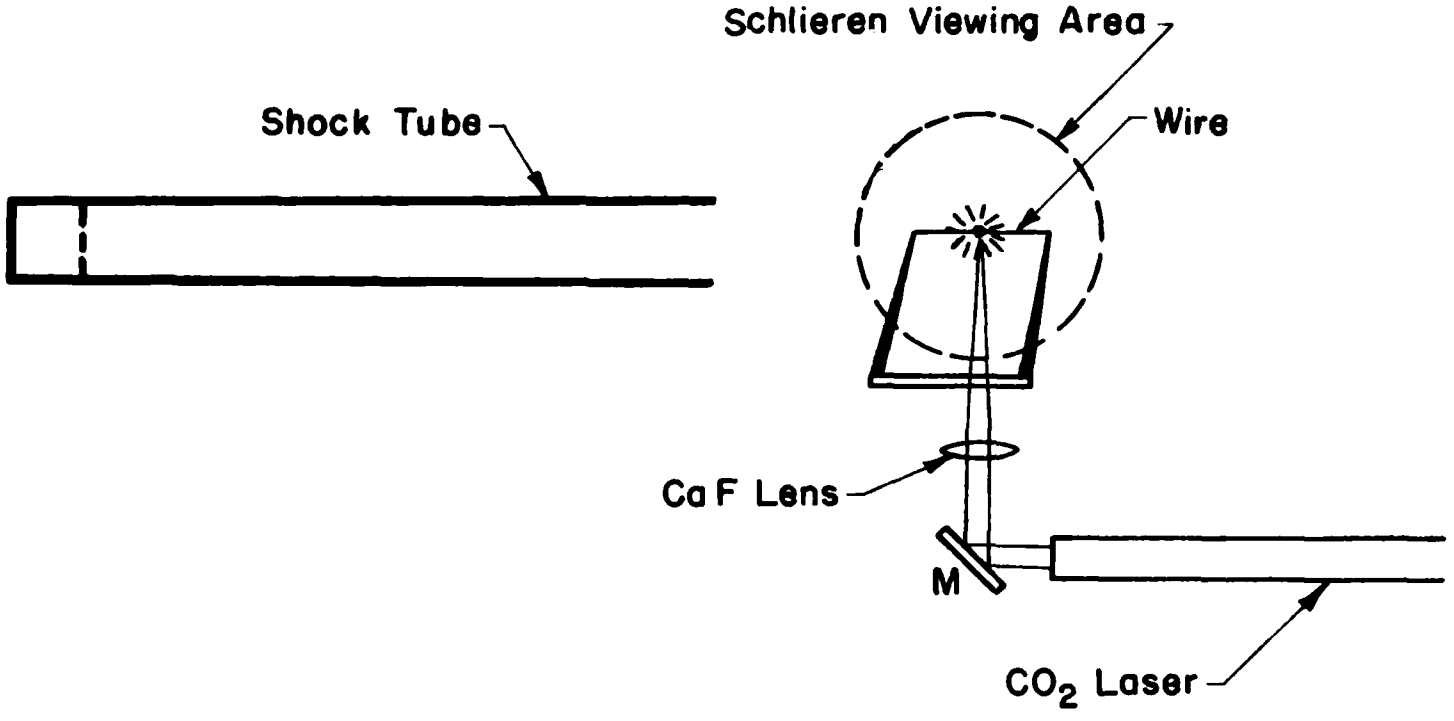

FIGURE 4 SCHEMATIC SIDE VIEW OF CO_2 LASER LAYOUT

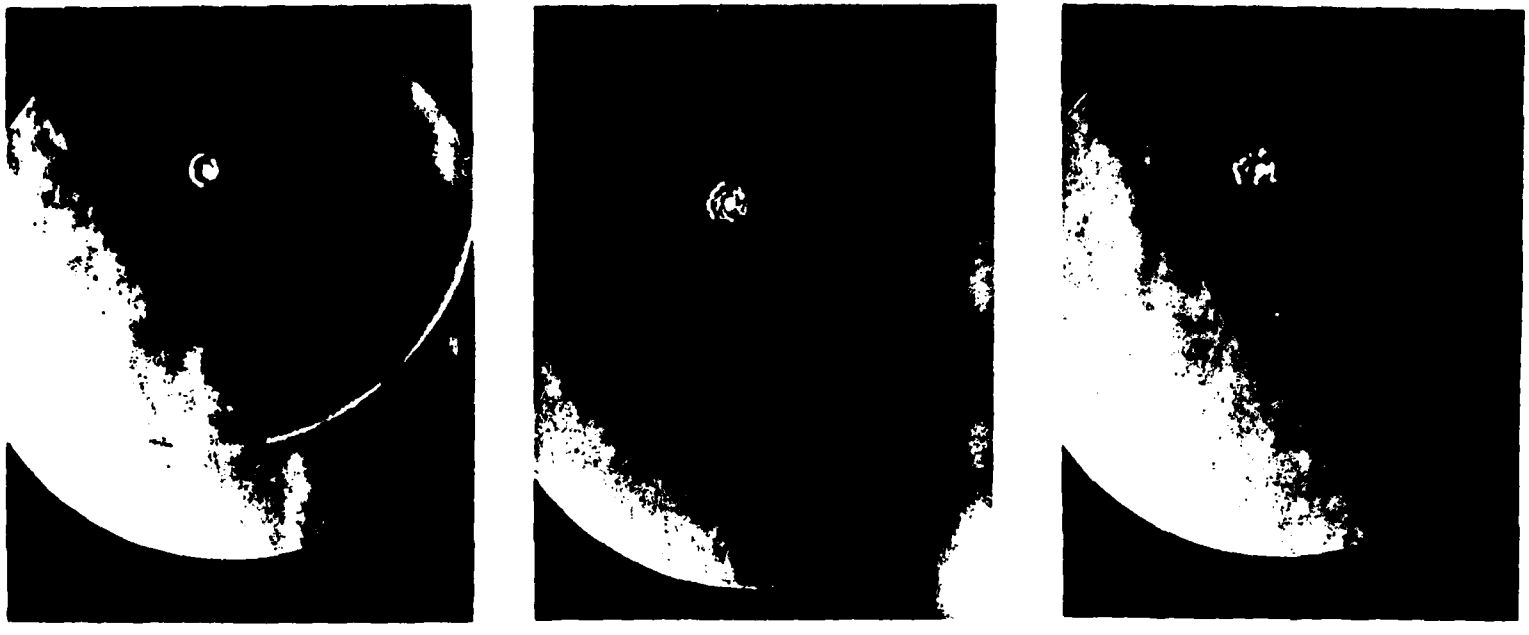

Figure 5. Schlieren Views of Laser Spark Tracer

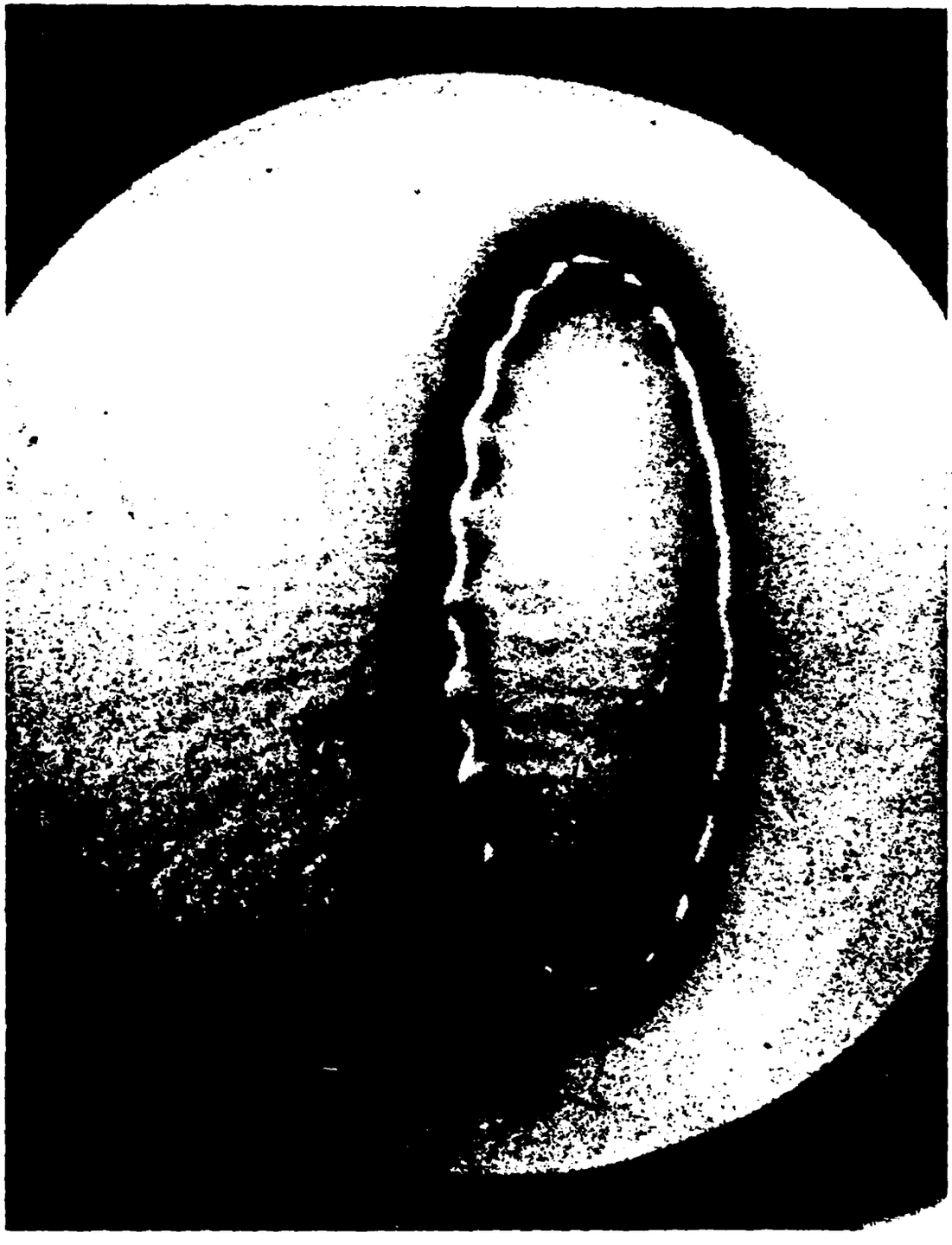

Figure 6. Ring Vortex Visualized by Schlieren Photography

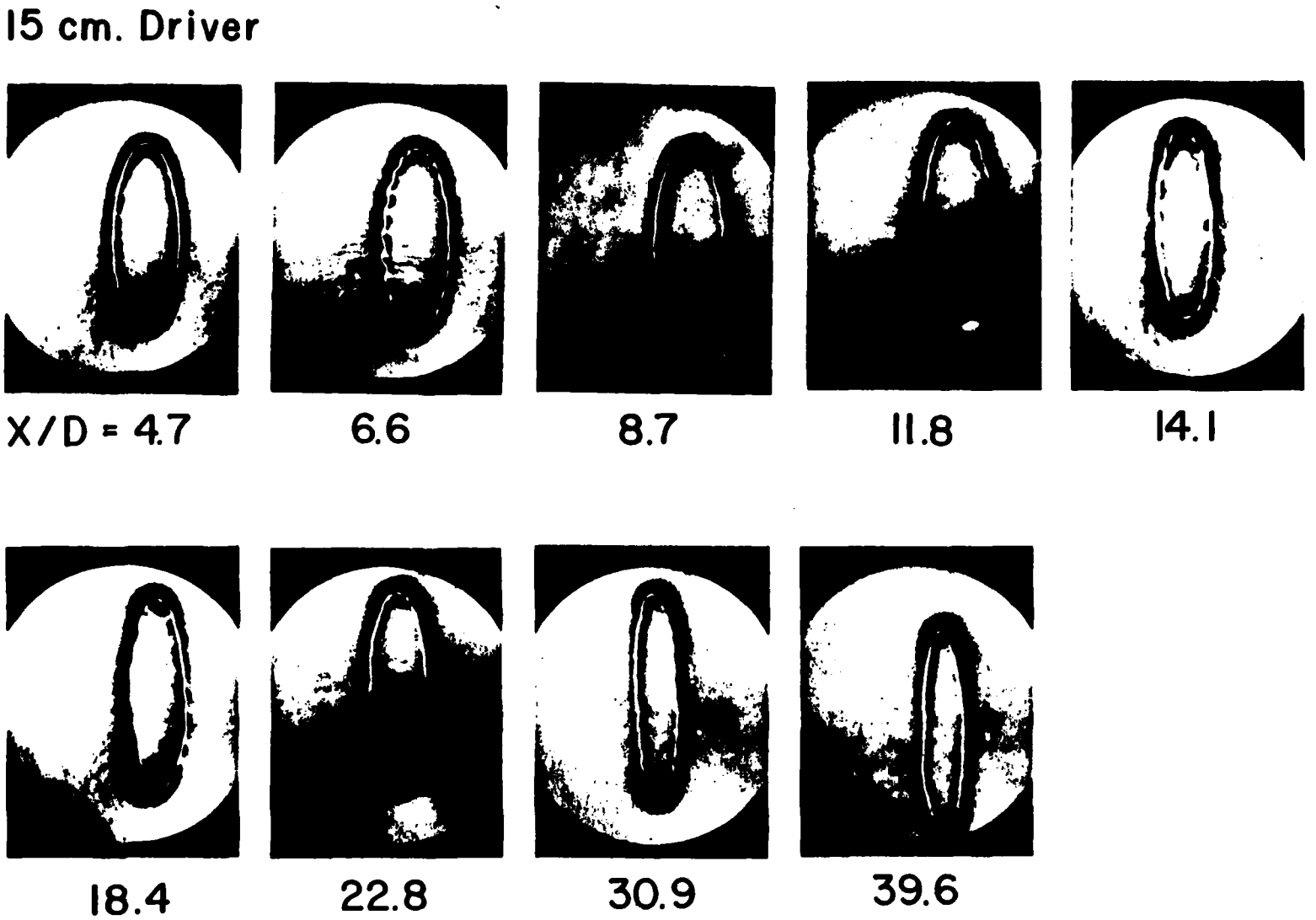

Figure 7. Schlieren Photographs of Ring Vortices
at Different Distances from Generator

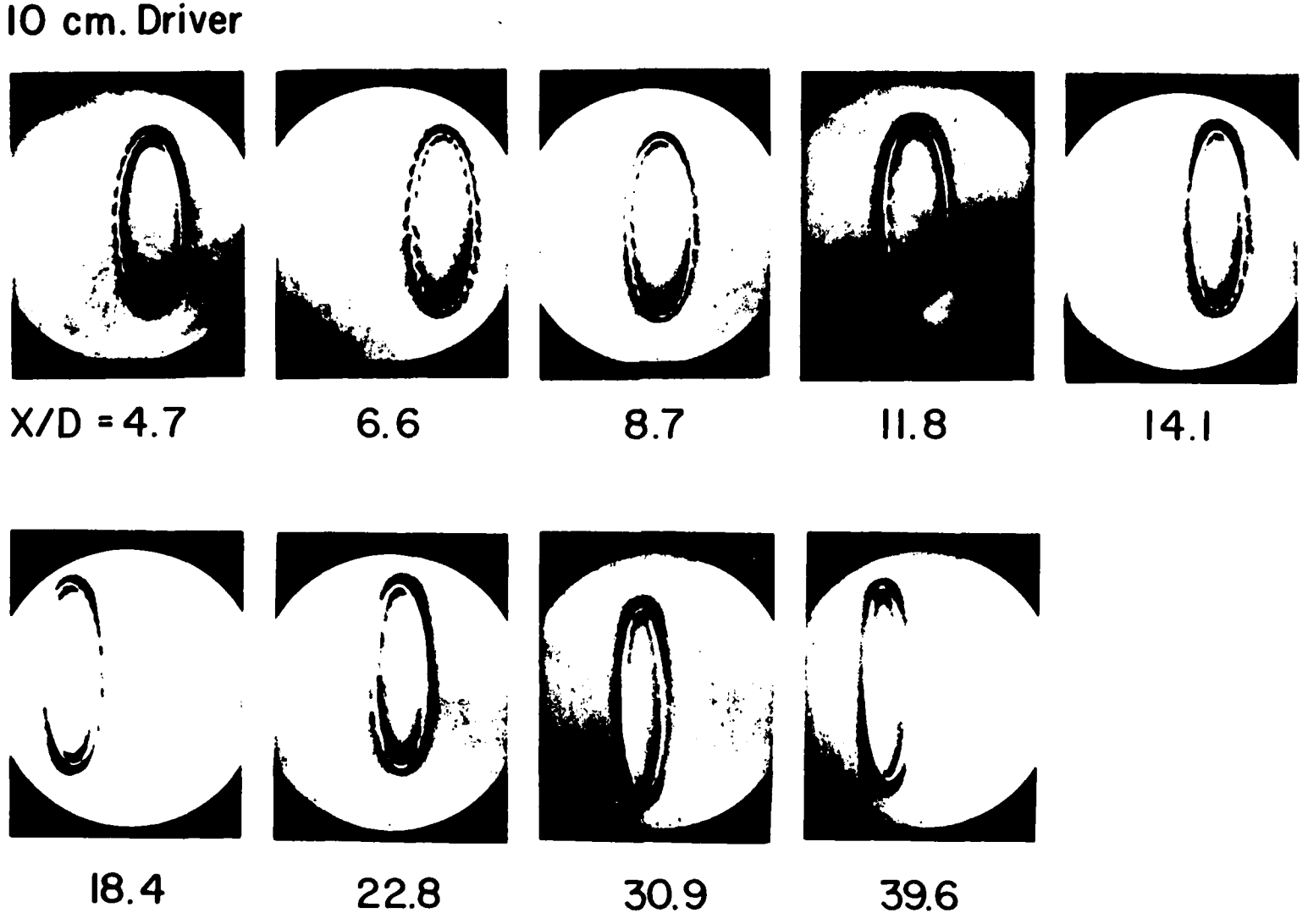

Figure 8. Schlieren Photographs of Ring Vortices
at Different Distances from Generator

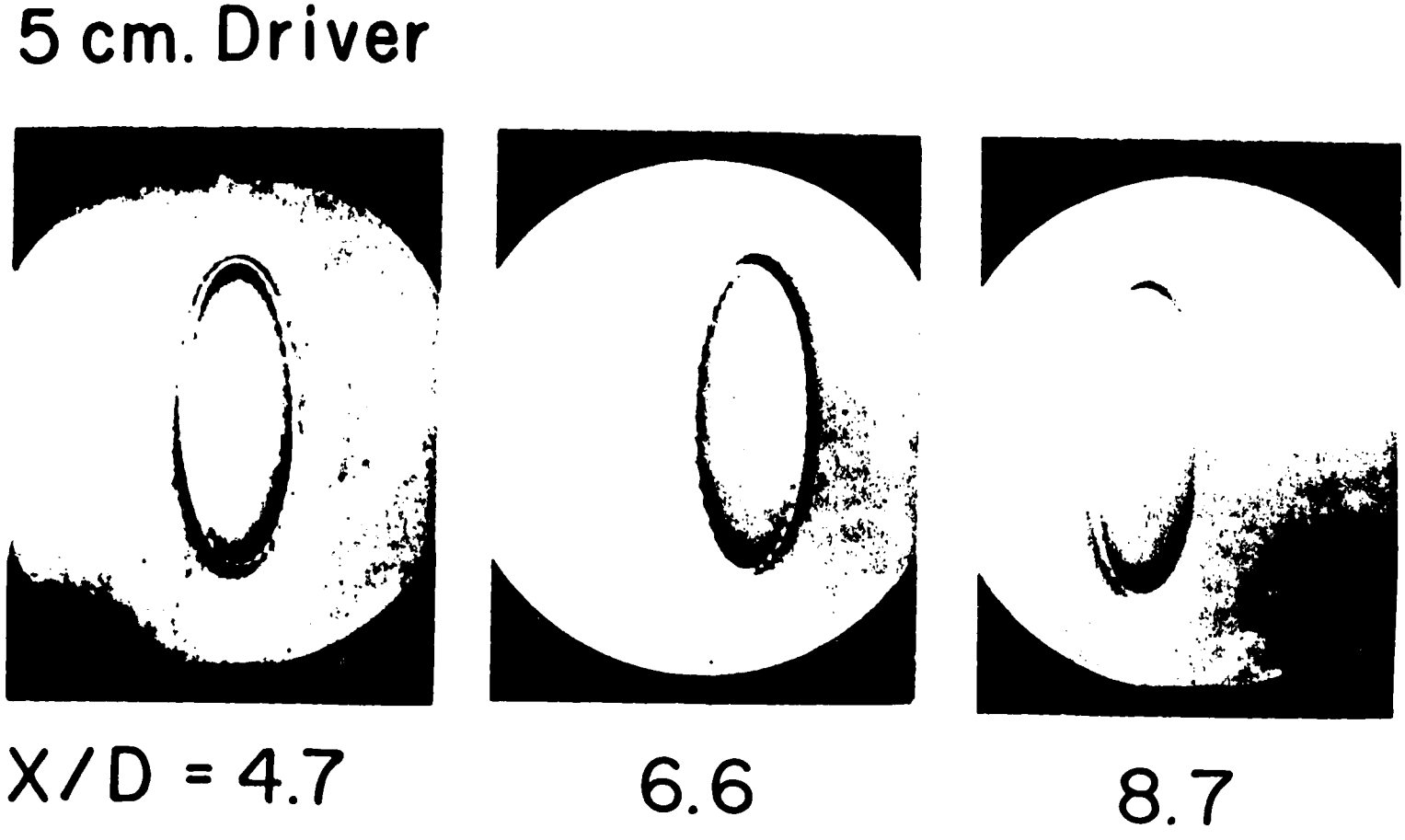

Figure 9. Schlieren Photographs of Ring Vortices
at Different Distances from Generator

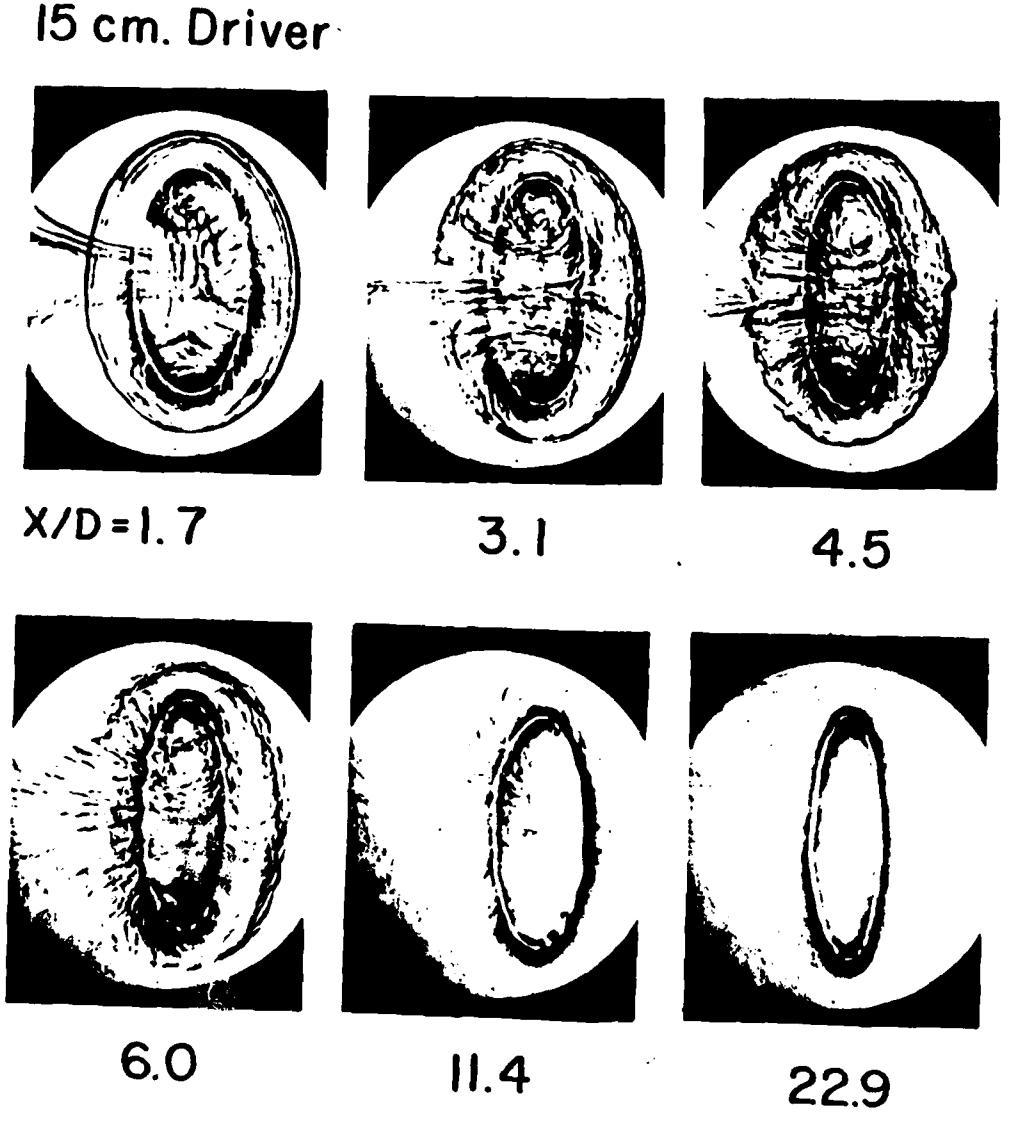

Figure 10. Schlieren Photographs of Ring Vortices with Cooled-Gas Visualization

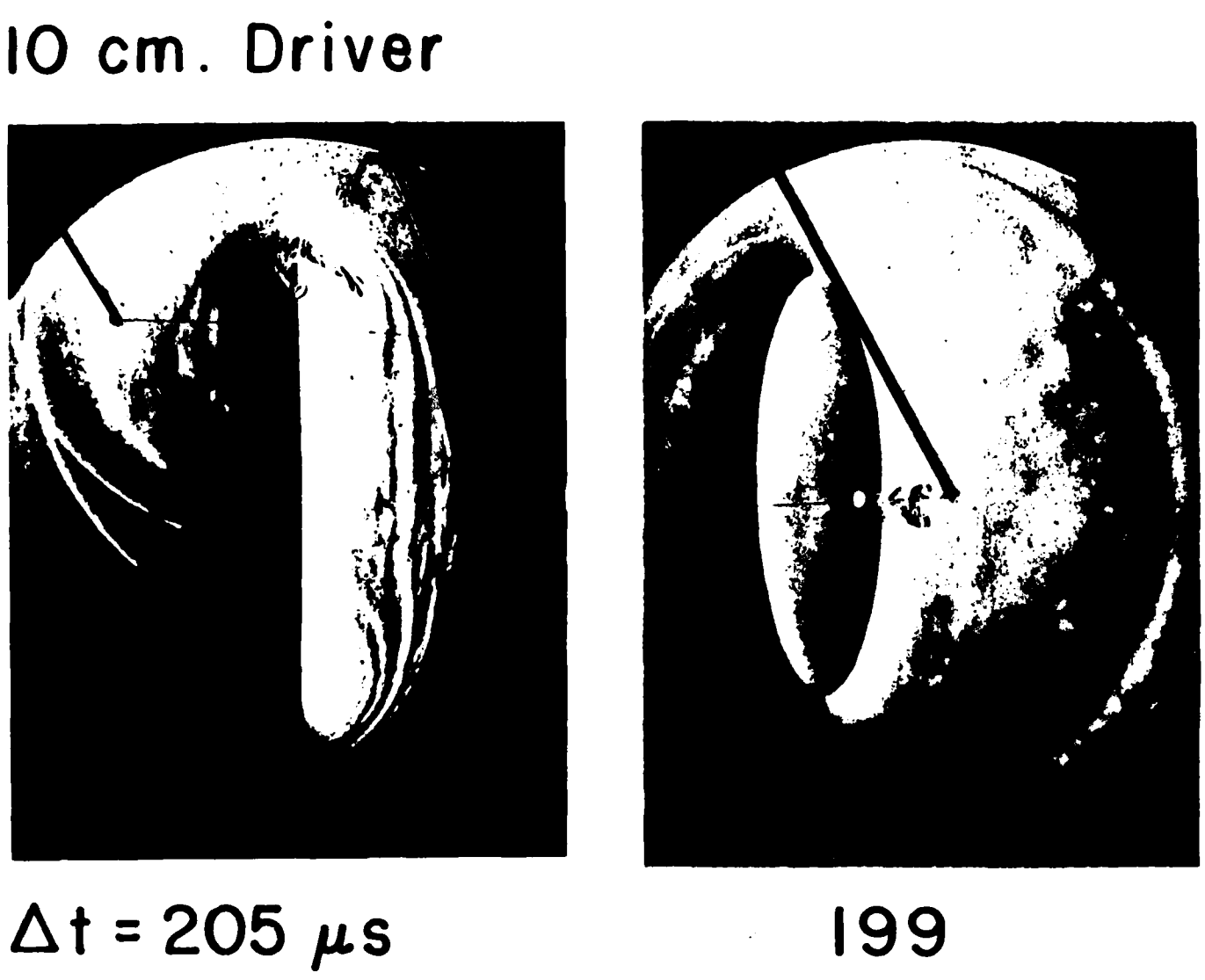

Figure 11. Side and Top Views of Distortion
of Laser Spark Tracer in Vortex Ring

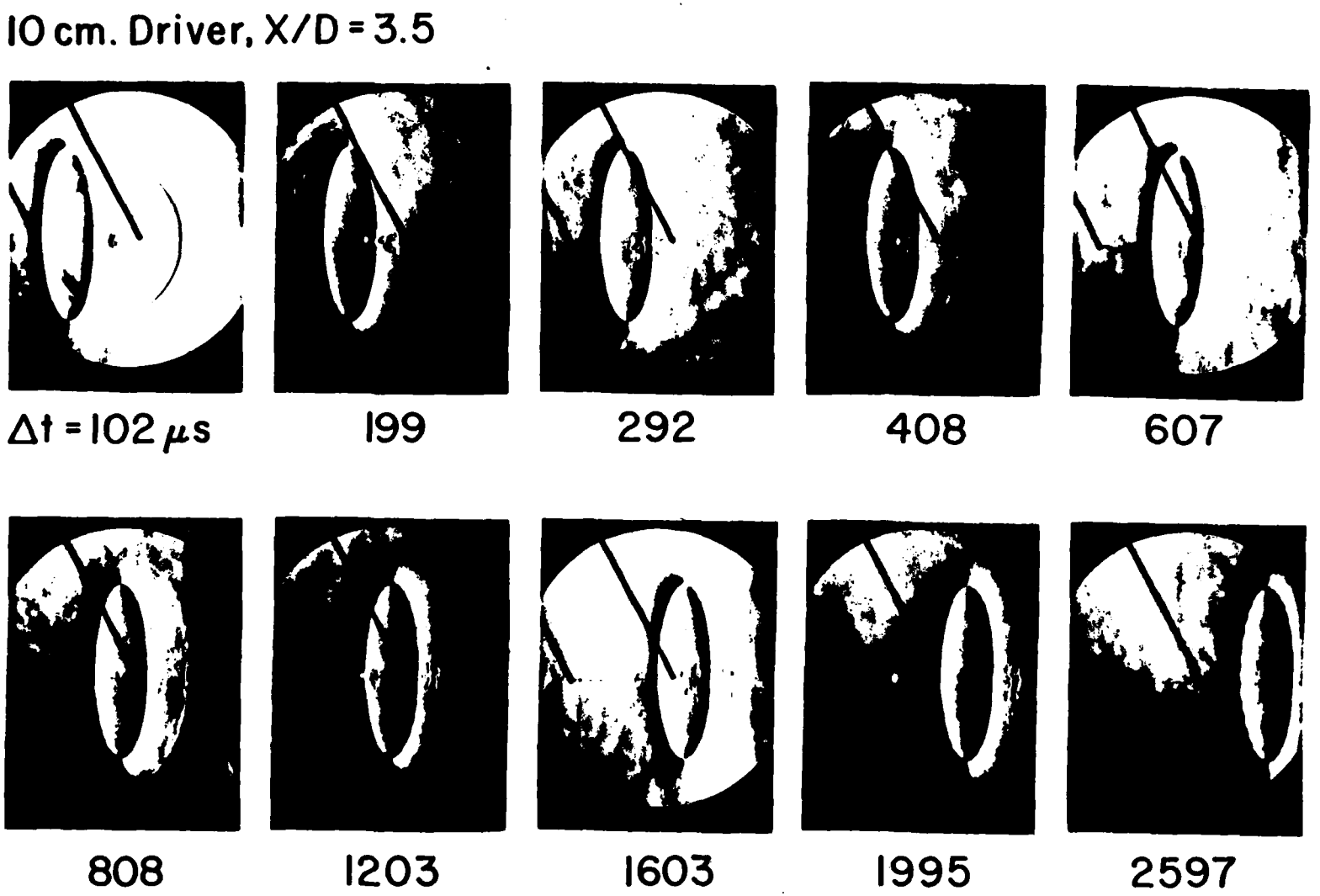

Figure 12. History of Laser Spark
Tracer Development in Vortex Ring

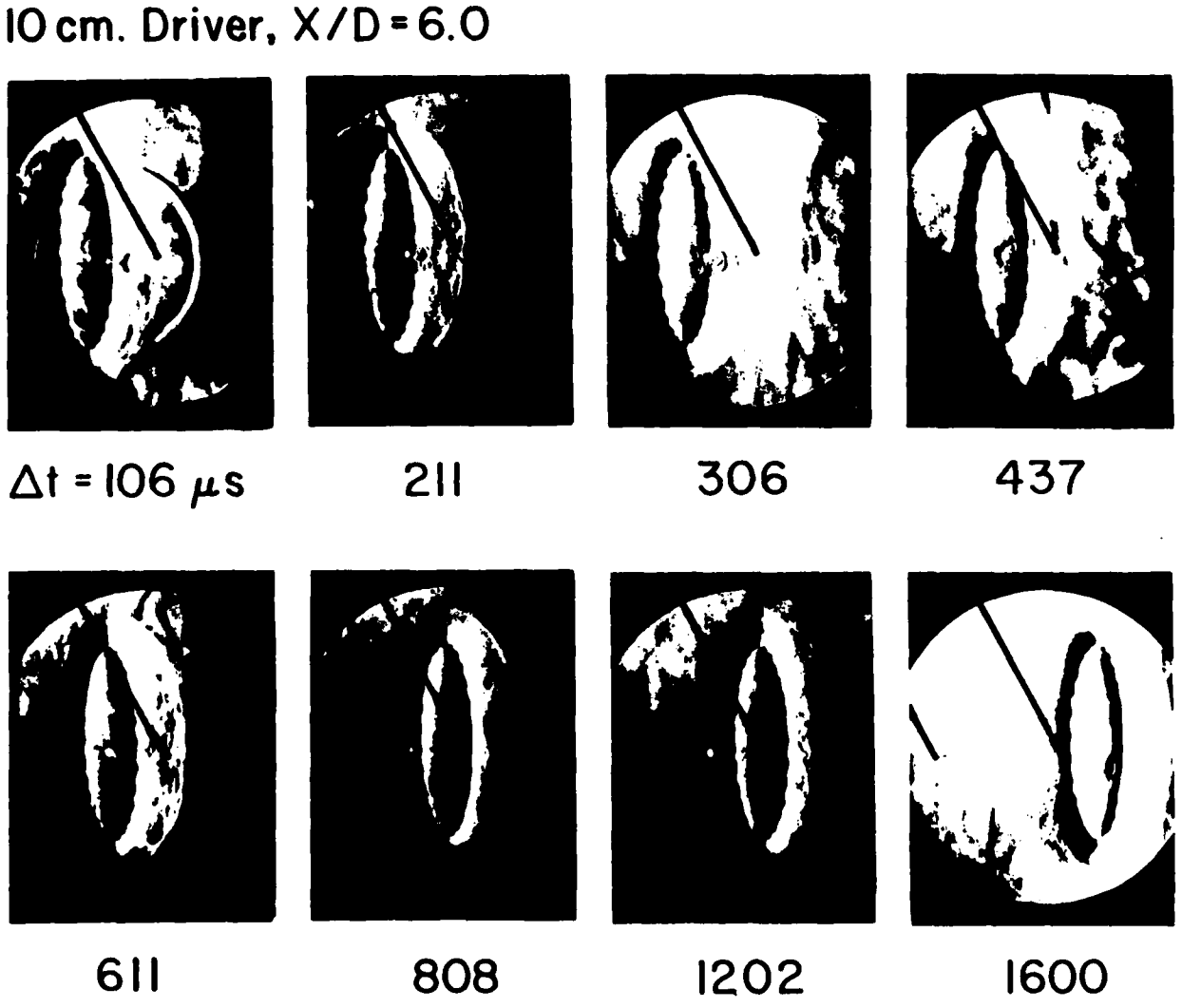

Figure 13. History of Laser Spark
Tracer Development in Vortex Ring

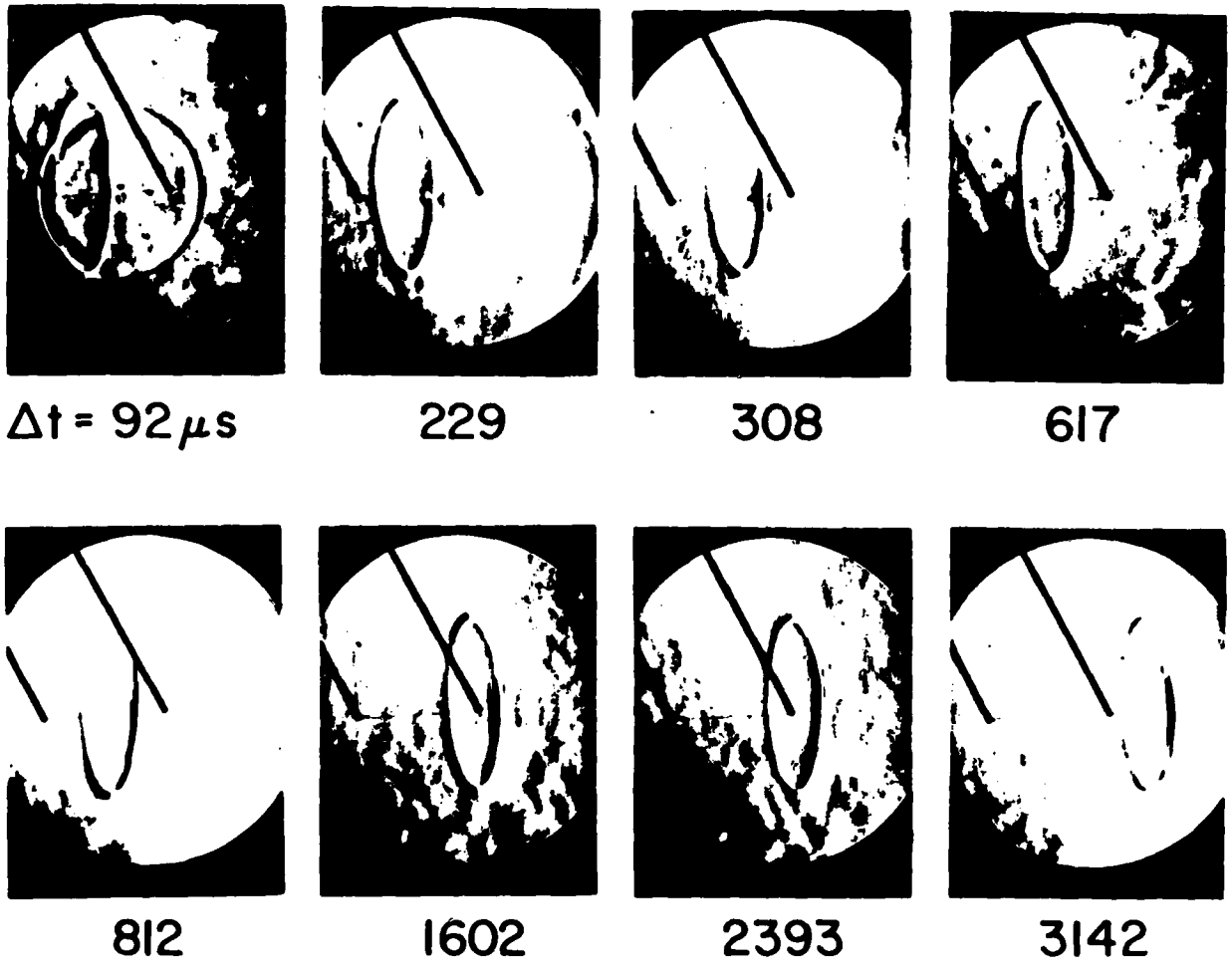

Figure 14. History of Laser Spark
Tracer Development in Vortex Ring


DAT
ILM